Atomic layer deposition of Al_2O_3 on V_2O_5 xerogel film for enhanced lithium-ion intercalation stability

Dawei Liu,[a] Yanyi Liu, Stephanie L. Candelaria, and Guozhong Cao[b]
Department of Materials Science and Engineering, University of Washington, Seattle, Washington 98195

Jun Liu
Pacific Northwest National Laboratories, 902 Battelle Boulevard, P.O. Box 999, Richland, Washington 99352

Yoon-Ha Jeong
National Center for Nanomaterials Technology, Pohang University of Science and Technology, Pohang, South Korea

(Received 16 August 2011; accepted 3 November 2011; published 29 November 2011)

V_2O_5 xerogel films were fabricated by casting V_2O_5 sols onto fluorine-doped tin oxide glass substrates at room temperature. Five, ten and twenty atomic layers of Al_2O_3 were grown onto as-fabricated films respectively. The bare film and Al_2O_3-deposited films all exhibited hydrous V_2O_5 phase only. Electrochemical impedance spectroscopy study revealed increased surface charge-transfer resistance of V_2O_5 films as more Al_2O_3 atomic layers were deposited. Lithium-ion intercalation tests at 600 mAg^{-1} showed that bare V_2O_5 xerogel film possessed high initial discharge capacity of 219 $mAhg^{-1}$ but suffered from severe capacity degradation, i.e., having only 136 $mAhg^{-1}$ after 50 cycles. After deposition of ten atomic layers of Al_2O_3, the initial discharge capacity was 195 $mAhg^{-1}$ but increased over cycles before stabilizing; after 50 cycles, the discharge capacity was as high as 225 $mAhg^{-1}$. The noticeably improved cyclic stability of Al_2O_3-deposited V_2O_5 xerogel film could be attributed to the improved surface chemistry and enhanced mechanical strength. During repeated lithium-ion intercalation/de-intercalation, atomic layers of Al_2O_3 which were coated onto V_2O_5 surface could prevent V_2O_5 electrode dissolution into electrolyte by reducing direct contact between active electrode and electrolyte while at the same time acting as binder to maintain good mechanical contact between nanoparticles inside the film. © *2012 American Vacuum Society*. [DOI: 10.1116/1.3664115]

I. INTRODUCTION

Lithium-ion batteries become the focus of rechargeable batteries in the new decade. Its success in powering portable electronic devices such as cellular phones and laptops has raised strong interests in pushing its application in large mobile devices, e.g., hybrid vehicles.[1,2] The advantages of using Li-ion batteries as alternative of fossil fuel for hybrid vehicle power source lie not only in energy perspective but also in environmental considerations.[3,4] However, the application in hybrid vehicles requires high discharge capacity which current lithium-ion batteries do not have. Worldwide research has been carried out to improve the intercalation capabilities of lithium-ion battery electrodes in the past decade and a lot of inspiring results have been published on improving the discharge capacities.[5–7] It was reported that for some intercalation host, amorphous or less crystallized state could be more favorable for lithium ion intercalation, i.e., possessing higher discharge capacity, due to the less well packed structure and more freedom for lithium ion diffusion.[8–11] V_2O_5 is one of these materials: less crystallized hydrous V_2O_5 phase was found to accommodate more lithium ions as compared with well crystallized phase.[12,13] In addition, formation of hydrous V_2O_5 does not need thermal treatment in fabrication process so it could be more suitable to be used for novel film battery on conductive plastic substrate.[14] However, the capacity loss of hydrous V_2O_5 during the repeated lithium-ion insertion/extraction process is also severe.[15] This phenomenon is attributed to two major reasons. The first one is the dissolution of electrode in the electrolyte, especially for nanostructured and poor crystallized materials whose surface area was often much larger than bulk and well crystallized materials.[16] the second one is related with the poor mechanical strength of un-annealed electrodes[17]: Electrodes without thermal annealing or other special treatment often suffer from poor mechanical strength and thus could lose contact between particles more easily. During the repeated lithium-ion insertion/extraction process, nanoparticles in the film could easily fall apart and the interconnection inside the electrode is severely damaged.[18] To solve these two problems, nano-sized coating of oxides is often used. They can modify the electrode surface chemistry while at the same time increasing the mechanical strength of the film electrode.[19,20] However, nano-sized coating is often realized by employing solution-based route and conformal coating ontoporous electrode is especially difficult due to the capillary force associated with mesopores and micropores resisting liquid penetration.[21,22] Atomic layer deposition (ALD) turns out

[a]Present address: School of Engineering, Brown University, Providence, RI 02912.
[b]Author to whom correspondence should be addressed; electronic mail: gzcao@u.washington.edu

to be a favorable novel route to replace solution-based coating when applied on highly porous electrodes due to its gas-phase reaction mechanism.[23] Conformal atomic-thickness coating could be achieved via this method on the surface of porous films without changing any internal structure. Moreover, coating thickness could be easily controlled by choosing the appropriate number of deposition cycles. In this work, we employ ALD equipment to grow thin atomic layers of Al_2O_3 on the surface of less crystallized V_2O_5 xerogel film prepared at room temperature. After Al_2O_3 atomic layer deposition, it is found that the lithium-ion intercalation cyclic stability of V_2O_5 film is obviously improved as compared with bare film without Al_2O_3 deposition. This cyclic stability improvement is attributed to the binding role of Al_2O_3 atomic layers and also their protection of the electrode from dissolution in the electrolyte.

II. EXPERIMENT

A diluted sol of $V_2O_5 \bullet nH_2O$ was prepared using the method reported by Fontenot *et al.*[24] In brief: 0.136 g V_2O_5 powder was dissolved in 2 mL de-ionized water and 0.603 mL 30% H_2O_2 solution. The suspension was stirred until the V_2O_5 powder totally dissolved, resulting in a clear and dark-red solution. The solution was then sonicated to get a yellow-brown gel which was dispersed into de-ionized water in a molar concentration of 0.005 M with primary vanadium species in the colloidal dispersion nanoparticles of hydrated vanadium oxide. $V_2O_5 \bullet nH_2O$ films were then prepared by spreading 50 μL of $V_2O_5 \bullet nH_2O$ sol onto fluorine-doped tin oxide glass substrates. The spread area was approximately 7 mm * 8 mm. After drying under ambient conditions for 24 hs, the films were then treated by atomic layer deposition (Oxford OpAL) of Al_2O_3 under vacuum at 25 °C for zero, five, ten and twenty cycles, respectively. The resultant films were designated as bare V_2O_5, Al_2O_3-5, Al_2O_3-10 and Al_2O_3-20.

Scanning electron microscopy (SEM, Philips, JEOL JSM7000) and x ray diffraction (XRD, Philips 1820 x ray diffractometer) were carried out to characterize the morphology and crystallization state of as-fabricated films. Electrochemical impedance spectroscopy (EIS) study was carried out using a Salon 1260 impedance/gain-phase analyzer with a Pt foil as the counter electrode and 1 M $LiClO_4$ in propylene carbonate as the electrolyte. The frequency range was from 100 kHz to 0.1 Hz. Lithium-ion intercalation properties of V_2O_5 films were investigated using a standard three-electrode system, with 1 M $LiClO_4$ in propylene carbonate as the electrolyte, a Pt mesh as the counter electrode, and Ag/AgCl as the reference electrode. Cyclic voltammetric (CV) tests were conducted between 0.6 V and −1.4 V with a scan rate of 10 mVs^{-1}. Chronopotentiometric (CP) tests were carried out in the voltage range from 0.6 V to −1.4 V with current density of 600 mAg^{-1}. The CV and CP tests were performed using an electrochemical analyzer (CH Instruments, Model 605B). The area of the working electrode used for all the electrochemical studies was 7 mm × 8 mm approximately.

III. RESULTS AND DISCUSSIONS

A. Results

The as-fabricated sol-gel film was homogeneous and SEM study (not shown here) revealed plain surface morphology with film thickness of ~2 μm. After atomic layer deposition, no noticeable morphology change was observed. As reported earlier, such xerogel film was highly porous with porosity ca. 50%.[13] The high porosity could be attributed to the solution-based route without thermal treatment. Water residues trapped in the pores can be removed by high vacuum processing during atomic layer deposition. Crystal water bonded to V_2O_5 structure is estimated to be 0.7 H_2O per V_2O_5 by TGA measurement. X-ray diffraction pattern of as-fabricated film is shown in Fig. 1. The broad peak discerned on the pattern is (0 0 1) peak of hydrous V_2O_5 phase and the interlayer distance between adjacent layers is 11.7 Å by calculation using the diffraction angel of (0 0 1) peak; the crystallite size estimated by using Scherrer's formula is ca. 5 nm, which is the thickness of the platelet along <0 0 1> direction. No crystallography change is observed on XRD patterns after different cycles of atomic layer deposition of Al_2O_3, suggesting that the crystal water remains bonded in the structure without being affected by high vacuum process.

The EIS of all the films are presented in Fig. 2. Figure 2(a) shows the high to middle frequency region of Nyquist plots (it is only part of the measured Nyquist plots) of the measured films and Fig. 2(b) shows the equivalent circuit that was used for fitting the measured Nyquist plots. In Fig. 2(b)'s circuit, R_1 represents the resistance of electrolyte; R_2 is the charge-transfer resistance of V_2O_5 film; R_3 represents the resistance of V_2O_5 film (or the electrode); and the CPEs in the circuit are constant phase elements.[25] Electrolyte resistance of the films reveals the process of lithium ion transport in the electrolyte and its value is the resistance value that the Nyquist plot semicircle starts from. It can be noticed that Al_2O_3 coated films all have lower electrolyte resistance (~120 Ω) than bare V_2O_5 (~180 Ω). Similar electrolyte resistance decrease after coating was also reported on Al_2O_3 coated $LiCoO_2$ (Ref. 26) and $AlPO_4$

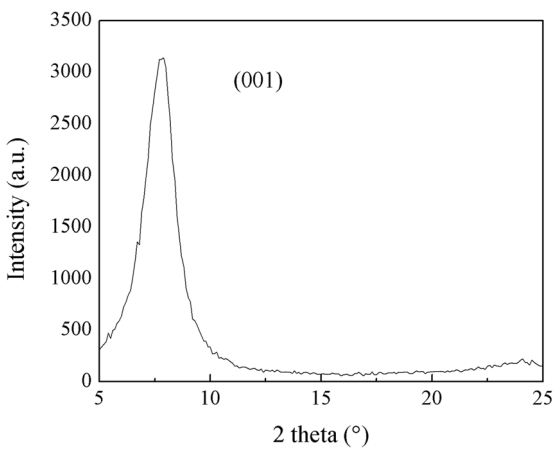

FIG. 1. X-ray diffraction pattern of V_2O_5 xerogel film fabricated at room temperature, showing the existence of only hydrous vanadium oxide.

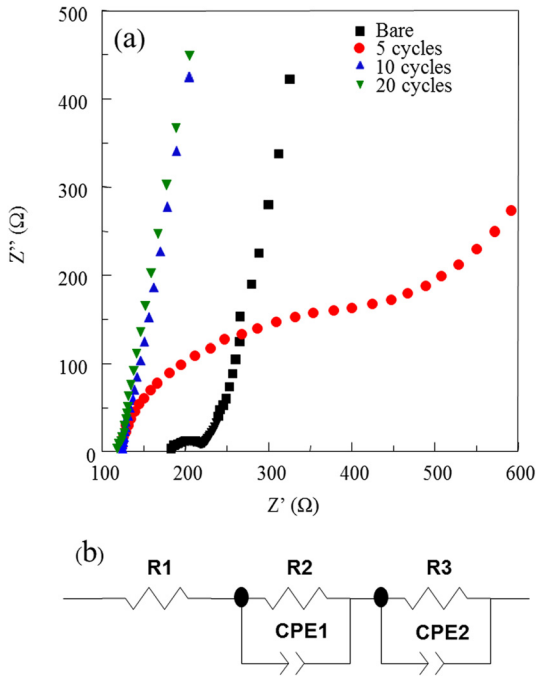

FIG. 2. (Color online) (a) High to middle frequency region of AC impedance spectra presented as Nyquist plots of bare V_2O_5 film and V_2O_5 films after Al_2O_3 deposition of different cycles measured in 1 M $LiClO_4$ in propylene carbonate and (b) the equivalent circuit used to fit the EIS data.

coated electrode.[27] Charge-transfer resistance reveals the process of lithium ion charge-transfer across the electrolyte/electrode interface. As could be clearly seen after the comparison of the Nyquist plots of the four films, with more Al_2O_3 cycles deposited, the semicircle representing the charge-transfer resistance becomes larger. The charge-transfer resistance values after fitting the Nyquist plots with the equivalent circuit shown in Fig. 2(b) show increasing magnitude: Bare V_2O_5 (68 Ω) < Al_2O_3-5 (400 Ω) < Al_2O_3-10 (2.9 kΩ) < Al_2O_3-20 (4.7 kΩ). It should be noted that as more Al_2O_3 atomic layers are deposited, the charge-transfer resistance exhibits noticeable increase which is due to more inert and insulating Al_2O_3 on V_2O_5 film surface.

The lithium-ion intercalation properties of all the films were studied using cyclic voltammetric (CV) and chronopotentiometric (CP) tests. Figure 3 compares the CV curves of the four films in the first, thirtieth and fiftieth cycles. For bare V_2O_5 film, the initial CV curve exhibits broad oxidation and reduction peaks, suggesting poor crystallinity of the film.[28] Reduction peaks are associated with lithium ion insertion reaction:

$$V_2O_5 + xLi^+ + xe^- = Li_xV_2O_5. \quad (1)$$

Oxidations peaks are associated with lithium ion extraction reaction:

$$Li_xV_2O_5 = V_2O_5 + xLi^+ + xe^-. \quad (2)$$

There are two pairs of redox peaks from bare V_2O_5 film with the more noticeable pair appearing at − 0.76 V (reduction peak) and − 0.39 V (oxidation peak) and the less noticeable ones at −0.21 V (reduction peak) and 0.15 V (oxidation peak). There is another oxidation peak at −0.25 V, but the peak disappears very quickly after initial cycles which could

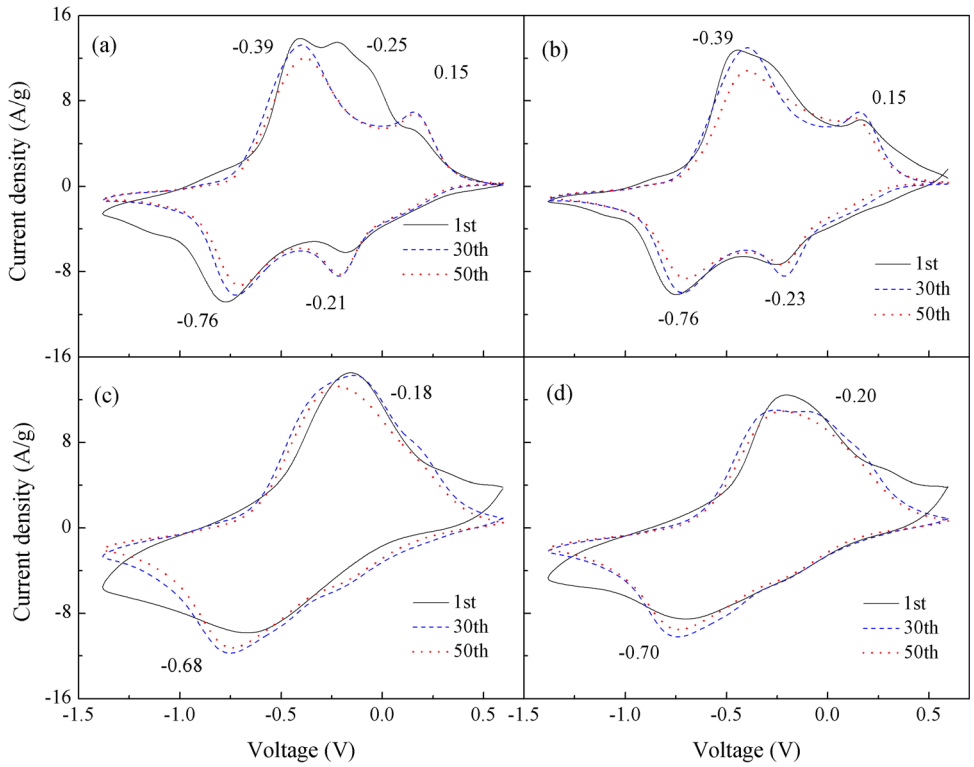

FIG. 3. (Color online) Cyclic voltammetry curves in the first, thirtieth and fiftieth cycles of (a) bare V_2O_5 film, (b) Al_2O_3-5 film, (c) Al_2O_3-10 film, and (d) Al_2O_3-20 film measured in 1 M $LiClO_4$ in propylene carbonate with a scan rate of 10 mVs^{-1} in a voltage range between 0.6 V and − 1.4 V vs Ag/AgCl.

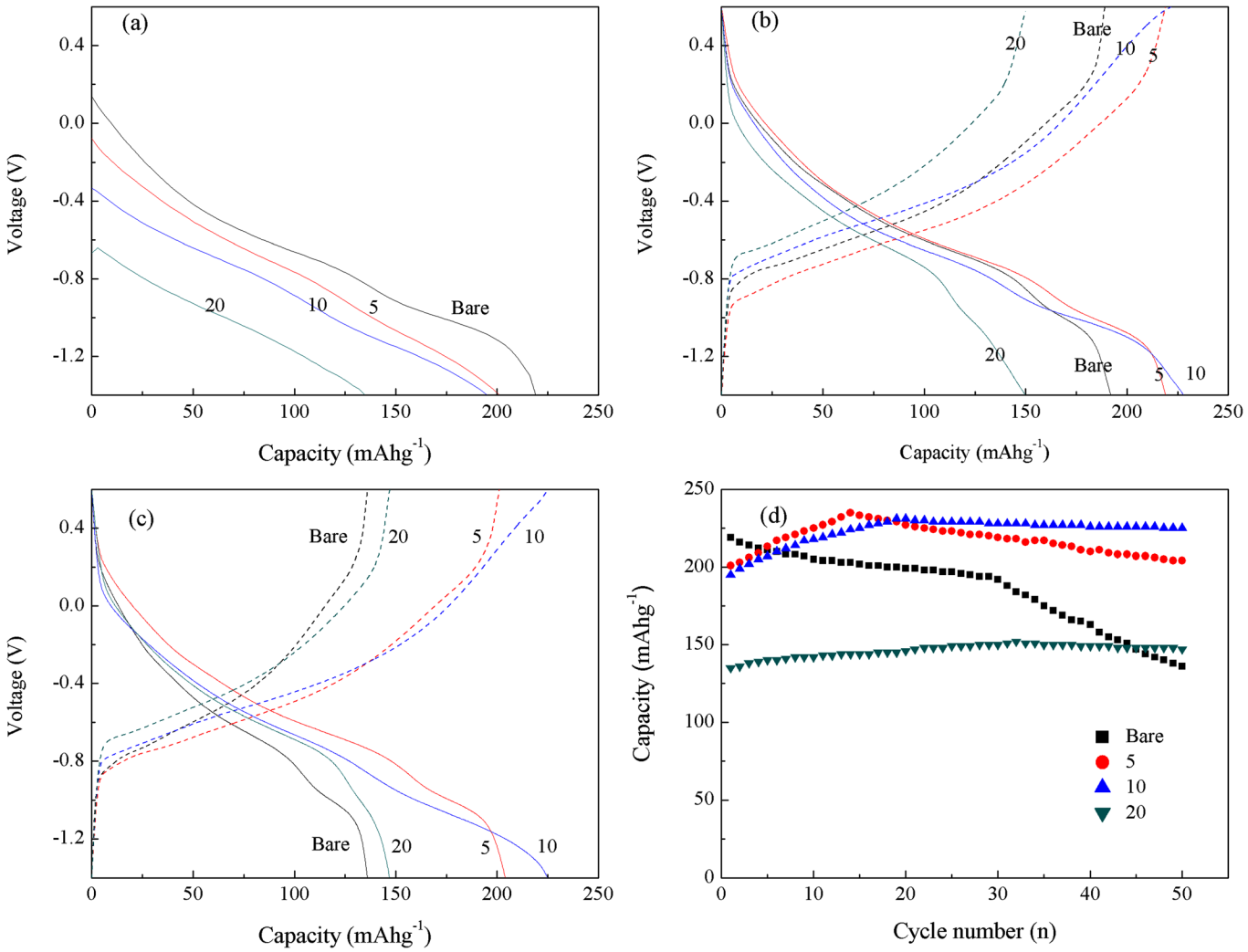

FIG. 4. (Color online) Chronopotentiometric discharge/charge curves in the (a) first, (b) thirtieth, and (c) fiftieth cycles of bare V_2O_5 film and Al_2O_3 deposited films. (d) Li-ion intercalation discharge capacity of bare V_2O_5 film and Al_2O_3 deposited films as a function of cyclic numbers. The measurements were carried out in a potential window between 0.6 V and −1.4 V vs Ag/AgCl at a current density of 600 mAg^{-1}.

be from surface impurities present due to absence of thermal treatment. The CV curve of Al_2O_3-5 film exhibits similar curve shape and peak positions as bare V_2O_5 film. However, the impurity peak at −0.25 V becomes much less noticeable, suggesting improved surface purity. The CV curves of Al_2O_3-10 and Al_2O_3-20 only exhibit one pair of redox peaks at −0.68 V (reduction peak) and -0.18 V (oxidation peak) in the initial cycle. With cycles going on, the peaks at −0.21 V and 0.15 V start to form, suggesting more V_2O_5 redox reaction with electrolyte. This phenomenon suggests that deposition of Al_2O_3 atomic layers on V_2O_5 surface suppresses the interface reactions in the initial cycles, including both the lithium-ion intercalation and minor side reactions. However, after stabilization of electrode/electrolyte interphase, more lithium-ion intercalation reactions start to occur.

Figures 4(a)–(c) show the discharge/charge curves of the four films. Figure 4(a) compares their initial discharge curves. It could be clearly seen that as more Al_2O_3 atomic layers are deposited, the starting voltage of discharge curve is getting lower and the discharge capacity is obviously decreasing. In detail, bare V_2O_5 film starts voltage drop from 0.17 V and has a high discharge capacity of 219 $mAhg^{-1}$; its discharge curve also exhibits two poorly-defined plateaus from −0.5 V to −0.7 V and from −0.9 V to − 1.1 V. After deposition of 5 Al_2O_3 atomic layers, the discharge curve starts voltage drop from −0.08 V and the initial capacity decreases to 201 $mAhg^{-1}$; the initial voltage of Al_2O_3-10 film further lowers to −0.35 V and capacity reduces to 195 $mAhg^{-1}$; Al_2O_3-20 film starts the voltage drop from −0.52 V and has an initial capacity of merely 135 $mAhg^{-1}$. Figures 4(b) and 4(c) compare the discharge/charge curves of these four films after 30 and 50 cycles. Compared with the discharge curves in Fig. 4(a), we could notice that bare V_2O_5 film has the highest discharge capacity in the initial cycle; however, after 30 cycles, it exhibits noticeable capacity decrease while the Al_2O_3 deposited films exhibit capacity increase. After 50 cycles, the bare V_2O_5 has a poor capacity of ∼130 $mAhg^{-1}$, and the Al_2O_3 deposited films all have higher capacities. All the films, whether bare V_2O_5 or Al_2O_3 deposited films, exhibits good columbic efficiency by delivering nearly the same charge capacity as discharge capacity, indicating good reversibility of lithium-ion

intercalation/de-intercalation process. The lower starting voltage of Al_2O_3 deposited V_2O_5 suggests less direct contact between electrolyte and active V_2O_5 electrode.[29] Another finding from the CP curves comparison is that V_2O_5 films deposited by Al_2O_3 exhibit more sloping intercalation manner in the initial cycles; however, after repeated cycles, poorly-defined plateaus start to appear in similar voltage region as those discerned in the curves of bare V_2O_5 film. The same phenomenon was also reported on Al_2O_3 deposited silicon oxycarbide.[30]

Figure 4(d) compares the long-term cyclic stability of the four films by presenting the discharge capacities versus cycle numbers. The bare V_2O_5 film starts with a high capacity of 219 $mAhg^{-1}$ but dropped cycle by cycle to only 136 $mAhg^{-1}$ after 50 cycles. Al_2O_3-5 film starts with a slightly lower capacity of 201 $mAhg^{-1}$ but exhibits capacity increase in the initial cycles and is still as high as 204 $mAhg^{-1}$ after 50 cycles. The initial capacity increase is similar as what been reported on Al_2O_3 coated $LiCoO_2$.[31] Al_2O_3-10 film exhibits a more noticeable trend of initial increase by increasing from initial capacity of 195 $mAhg^{-1}$ to 225 $mAhg^{-1}$ after 50 cycles. Al_2O_3-20 film's behavior in the cyclic stability is similar as Al_2O_3-10 film but shows lower capacities through all the 50 cycles: it starts with a low capacity of 135 $mAhg^{-1}$ and stabilizes at 147 $mAhg^{-1}$ after 50 cycles. As demonstrated in the experiments, V_2O_5 film deposited with five or ten atomic layers of Al_2O_3 exhibited high discharge capacities with noticeably improved cyclic stability. When more than ten atomic layers of Al_2O_3 were deposited, the cyclic stability remained the same but the capacity value was much lower.

B. Discussions

The improved cyclic stability of V_2O_5 film after Al_2O_3 atomic layer deposition could be attributed to the enhanced surface chemistry stability and mechanical strength of V_2O_5 film. As reported by literature, electrode dissolution and volume change during the cyclic lithium-ion intercalation/de-intercalation process are the two main causes of capacity degradation.[32,33] Nanostructured films often deliver high capacities benefiting from the large surface contact area with electrolyte, providing sufficient reaction sites for lithium−ion intercalation. However, large interface also means more electrode dissolution in the electrolyte in long-term cycles, causing faster loss of active material and resultant capacity degradation. On the other hand, after lithium-ion intercalation, host film will experience volume expansion which often causes excessive mechanical stress, detrimental to the film structure integrity especially for unannealed films which suffer from poor mechanical strength. Coated atomic layers play the role both as the protection layer to reduce electrode dissolution into the electrolyte and also as binder to counter the volume change stress by holding reacting film more firmly.[34] Coating as the protection layer to protect electrode surface integrity has been widely recognized and it is already well proved to be highly effective as we discussed in the introduction part. However, the binding role of deposited atomic layers is not well recognized yet. For porous film, interconnected nanostructured particles are experiencing repeated volume expansion and could gradually lose contact between each other. As a result, the connection network is damaged and capacity degradation is evidenced. Thermal treatment could be one solution to solving the problem by increasing mechanical strength, i.e., building up more particle contact areas; however; at the same time, thermal treatment could also change the crystal structure and reduce total film surface area,[35] unfavorable for lithium-ion intercalation. In addition, in some advanced flexible energy storage device applications, due to the plastic substrate used for film battery, thermal treatment should also be avoided to ensure good substrate conductivity. In contrast to traditional thermal method, Al_2O_3 atomic layers increase film strength by acting as binders to hold expanding nanoparticles together during repeated cycles. Internal structure of the film can be well preserved and substrate conductivity will not be sacrificed. So ALD deposition is favorable as an effective method to increase film electrode mechanical strength.

IV. SUMMARY AND CONCLUSIONS

Atomic layers of Al_2O_3 were deposited onto sol-gel derived V_2O_5 xerogel films which did not receive any thermal treatment and lithium-ion intercalation capabilities of these films were studied. Bare V_2O_5 film had an initial discharge capacity as high as 219 $mAhg^{-1}$ but after 50 cycles its capacity was only 136 $mAhg^{-1}$. After Al_2O_3 deposition, the cyclic stability of V_2O_5 films was noticeably improved. The film deposited by five atomic layers of Al_2O_3 started with a capacity of 201 $mAhg^{-1}$ and after 50 cycles the capacity was still as high as 204 $mAhg^{-1}$; the film deposited by ten atomic layers of Al_2O_3 had an even better cyclic stability by starting with a lower capacity of 195 $mAhg^{-1}$ and after 50 cycles possessing a higher capacity of 225 $mAhg^{-1}$. The improved cyclic stability of V_2O_5 films after Al_2O_3 atomic layer deposition could be attributed to the inert Al_2O_3 layers both as the protection coating to reduce active electrode dissolution in the electrolyte and as the binders to increase the mechanical strength of the V_2O_5 film.

ACKNOWLEDGMENTS

This work was supported in part by National Science Foundation (Grant Nos. CMMI-1030048 and DMR-0605159). D.W.L. would like to acknowledge the graduate fellowship (UIF) from University of Washington Center for Nanotechnology (CNT). S.L.C. would like to acknowledge the NSF-IGERT fellowship (Grant No. DGE-0654252). Atomic layer deposition part of this work was conducted at the University of Washington NanoTech User Facility, a member of the NSF National Nanotechnology Infrastructure Network (NNIN).

[1]S. Bashash, S. J. Moura, J. C. Forman, and H. K. Fathy, J. Power Sources **196**, 541 (2011).
[2]W. Q. Lu, A. Jansen, D. Dees, P. Nelson, N. R. Veselka, and G. Henriksen, J. Power Sources **196**, 1537 (2011).

[3]M. R. Palacin, Chem. Soc. Rev. **38**, 2565 (2009).
[4]D. W. Liu and G. Z. Cao, Energy Environ. Sci. **3**, 1218 (2010).
[5]A. Yamada, N. Iwane, Y. Harada, S. I. Nishimura, Y. Koyama, and I. Tanaka, Adv. Mater. **22**, 3583 (2010).
[6]H. W. Lee, P. Muralidharan, R. Ruffo, C. M. Mari, Y. Cui, and D. K. Kim, Nano Lett. **10**, 3852 (2010).
[7]D. M. Yu, C. G. Chen, S. H. Xie, Y. Y. Liu, K. Park, X. Y. Zhou, Q. F. Zhang, J. Y. Li, and G. Z. Cao, Energy Environ. Sci. **4**, 858 (2011).
[8]W. T. Jeong, J. H. Joo, and K. S. Lee, J. Alloys Comp. **358**, 294 (2003).
[9]Y. Wang, K. Takahashi, K. Lee, and G. Z. Cao, Adv. Funct. Mater. **16**, 1133 (2006).
[10]Y. Y. Liu, D. W. Liu, Q. F. Zhang, D. M. Yu, J. Liu, and G. Z. Cao, Electrochim. Acta **56**, 2559 (2011).
[11]Y. Y. Liu, D. W. Liu, Q. F. Zhang, and G. Z. Cao, J. Mater. Chem. **21**, 9969 (2011).
[12]J. X. Wang, C. J. Curtis, D. L. Schulz, and J. G. Zhang, J. Electrochem. Soc. **151**, A1 (2004).
[13]D. W. Liu, Y. Y. Liu, B. B. Garcia, Q. F. Zhang, A. Q. Pan, Y. H. Jeong, and G. Z. Cao, J. Mater. Chem. **19**, 8789 (2009).
[14]L. B. Hu, H. Wu, F. L. Mantia, Y. Yang, and Y. Cui, ACS Nano **4**, 5843 (2010).
[15]Y. Wang and G. Z. Cao, Electrochim. Acta **51**, 4865 (2006).
[16]Y. Wang and G. Z. Cao, Adv. Mater. **20**, 2251 (2008).
[17]S. K. Soni, B. W. Sheldon, X. C. Xiao, and A. Tokranov, Scr. Mater. **64**, 307 (2011).
[18]B. J. Landi, M. J. Ganter, C. M. Schauerman, C. D. Cress, and R. P. Raffaelle, J. Phys. Chem. C **112**, 7509 (2008).
[19]C. Li, H. P. Zhang, L. J. Fu, H. Liu, Y. P. Wu, E. Ram, R. Holze, and H. Q. Wu, Electrochim. Acta **51**, 3872 (2006).
[20]A. Odani, V. G. Pol, S. V. Pol, M. Koltypin, A. Gedanken, and D. Aurbach, Adv. Mater. **18**, 1431 (2006).
[21]L. J. Fu, H. Liu, C. Li, Y. P. Wu, E. Rahm, R. Holze, and H. Q. Wu, Solid State Sci. **8**, 113 (2006).
[22]B. B. Garcia, D. W. Liu, S. Sepehri, S. Candelaria, D. M. Beckham, L. W. Savage, and G. Z. Cao, J. Non-Cryst. Solids **356**, 1620 (2010).
[23]K. Park, Q. F. Zhang, B. B. Garcia, X. Y. Zhou, Y. H. Jeong, and G. Z. Cao, Adv. Mater. **22**, 2329 (2010).
[24]C. J. Fontenot, J. W. Wiench, M. Pruski, and G. L. Schrader, J. Phys. Chem. B **104**, 11622 (2000).
[25]D. W. Liu, Y. Y. Liu, A. Q. Pan, K. P. Nagle, G. T. Seidler, Y. H. Jeong, and G. Z. Cao, J. Phys. Chem. C **115**, 4959 (2011).
[26]G. T. K. Fey, H. M. Kao, P. Muralidharan, T. P. Kumar, and Y. D. Cho, J. Power Sources **163**, 135 (2006).
[27]S. E. Lee, E. J. Kim, and J. P. Cho, Electrochem. Solid-State Lett. **10**, A1 (2007).
[28]Y. Wang and G. Z. Cao, Chem. Mater. **18**, 2787 (2006).
[29]Y. S. Jung, A. S. Cavanagh, L. A. Riley, S. H. Kang, A. C. Dillon, M. D. Groner, S. M. George, and S. H. Lee, Adv. Mater. **22**, 2172 (2010).
[30]D. J. Ahn and R. S. Raj, J. Power Sources **195**, 3900 (2010).
[31]I. D. Scott, Y. S. Jung, A. S. Cavanagh, Y. F. Yan, A. C. Dillon, S. M. George, and S. H. Lee, Nano Lett. **11**, 414 (2011).
[32]D. W. Liu, Q. F. Zhang, P. Xiao, B. B. Garcia, Q. Guo, R. Champion, and G. Z. Cao, Chem. Mater. **20**, 1376 (2008).
[33]R. Deshpande, Y. Qi, and Y. T. Cheng, J. Electrochem. Soc. **157**, A967 (2010).
[34]L. A. Riley, A. S. Cavanagh, S. M. George, Y. S. Jung, Y. F. Yan, S. H. Lee, and A. C. Dillon, ChemPhysChem **11**, 2124 (2010).
[35]D. M. Yu, S. T. Zhang, D. W. Liu, X. Y. Zhou, Q. F. Zhang, Y. Y. Liu, and G. Z. Cao, J. Mater. Chem. **20**, 10841 (2010).